Food Chemistry: X 24 (2024) 101837

Contents lists available at ScienceDirect

Food Chemistry: X

journal homepage: www.sciencedirect.com/journal/food-chemistry-x

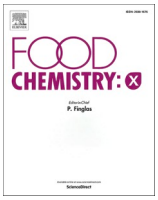

Enzymatic hydrolysis pretreatment combined with glycosylation for soybean protein isolate applying in dual-protein yogurt

Mengya Sun [a,1], Zhenhai Yu [b,1], Shuo Zhang [a], Caihua Liu [a], Zengwang Guo [a], Jing Xu [a], Guofang Zhang [a,*], Zhongjiang Wang [a,*]

[a] College of Food Science, Northeast Agricultural University, Harbin, Heilongjiang 150030, China
[b] Heilongjiang Province Green Food Science Institute, Harbin, Heilongjiang 150030, China

ARTICLE INFO

Keywords:
Enzymatic hydrolysis
Glycosylation
Soybean protein isolate
Dual-protein
Yogurt

ABSTRACT

This research investigated the viability of replacing milk protein with glycosylated soybean protein isolate (SPI) treated with different enzymatic hydrolysis times (0, 10, 20, 30, 40, and 50 min) in yogurt. The results showed that enzymatic hydrolysis pretreatment combined with glycosylation for SPI exhibited elevated grafting and solubility. Additionally, the high solubility of SPI (94.77 %) at 40 min facilitates the preparation of dual-protein yogurt (DPY). Compared to ESPI0-G, DPY that incorporates ESPI40-G through partial substitution of milk protein is capable of forming a denser and more stable gel matrix. Especially, the syneresis of DPY40 was reduced by 7.61 % compared to DPY0, which more closely approximates the texture properties of traditional yogurt. Meanwhile, glycosylated SPI treated with enzymatic hydrolysis can effectively degrade the beany flavor and slightly bitter taste in DPY. This study could provide a solid theoretical basis for the broader application and industrialization of plant-based yogurt.

1. Introduction

Recently, the dual-protein yogurt (DPY) product prepared by the combination of animal and plant proteins has become a research hot spot. Along with distinct texture and sensory properties, DPY provides more nutritional and functional benefits than single protein products. Consequently, more research teams have focused on combining animal and plant proteins to create new products. DPY can be prepared with many plant materials, such as soybeans, coconuts, rice, and oats, among others. However, the proliferation rate of lactic acid bacteria is limited to the availability of soluble carbohydrates and the solubility of plant-derived proteins utilized in the fermentation process. The formation of the gel system in yogurt mainly depends on the microbial acid production-mediated metabolism of sugar into lactic acid, resulting in a gradual reduction of pH to the isoelectric point of the protein. Meanwhile, the reduction of electrostatic repulsion between protein molecules promotes their aggregation, which leads to the formation of yogurt gels. Soybean protein isolate (SPI) is a complete protein with nutritional value comparable to milk protein. Meanwhile, SPI contains essential amino acids required by humans and has the closest ratio to human protein composition. Additionally, SPI is widely available because of its low prices. However, the gel structure resulting from fermentation using SPI as a substrate, characterized by limited molecular flexibility, is both rigid and fragile. Consequently, the limited structure of SPI hinders the formation of a gel with a desirable water holding capacity and robust toughness during fermentation. Additionally, the beany flavor of SPI severely limits the sensory quality of DPY, including its flavor and edible quality. Many studies have shown that particle size, changes in structure, and the degree of binding in the mixing system may affect the functional properties and flavor release of proteins (Shen et al., 2020). Therefore, the functional properties and flavor release capability of SPI are enhanced by modification, thereby making it more appropriate for DPY applications.

Currently, numerous modification techniques for regulating the spatial structure of SPI have been investigated to enhance its functional properties. These methods include heat treatment, ultrasound-assisted enzymatic hydrolysis, among others. Research has demonstrated that enzymatic hydrolysis and glycosylation treatment is effective in improving the processing properties of plant proteins during the fermentation of yogurt (Nanakali et al., 2023). The mechanism of

* Corresponding authors.
E-mail addresses: zgfandkenny@126.com (G. Zhang), wzjname@126.com (Z. Wang).
[1] These authors contributed equally to this work.

https://doi.org/10.1016/j.fochx.2024.101837
Received 27 May 2024; Received in revised form 10 September 2024; Accepted 13 September 2024
Available online 18 September 2024

enzymatic hydrolysis in enhancing the quality of plant-based yogurt primarily involves modifications to protein structure and size, the generation of peptides and amino acids, and the enhancement of flavor release (Ren & Li, 2022). Klost et al. (2020) observed that pea proteins, represented by globular proteins, can be broken down through enzymatic hydrolysis. This enzymatic hydrolysis process helps to weaken the rigid structure of proteins, subsequently promoting the formation of a dense gel network during acidification. Thus, syneresis in yogurt is effectively mitigated. Panyam and Kilara (1996) showed that limited enzymatic hydrolysis improved the gel structure in an acid-induced environment by reducing the molecular mass, increasing the number of ionized groups, and exposing previously embedded hydrophobic groups. Meanwhile, enzymatic hydrolysis can disrupt the firm binding of substances such as hexanal with terminal amino and carboxyl groups in proteins, removing the bad flavor more easily (Surrey, 1964). Moreover, the interaction between hydrophilic polysaccharides and proteins leads to the introduction of hydroxyl chains and consumption of amino groups, thereby altering the balance between hydrophilic and hydrophobic groups. This process synergizes with protein gelation, ultimately enhancing the quality of protein gels. Ke and Li (2023) reported that glycosylation changes the protein structure, resulting in the exposure of hydrophobic groups. This exposure promotes hydrophobic interactions between protein molecules, thereby enhancing their aggregation and cross-linking behavior during gel formation. Meanwhile, the covalent bonds formed during the glycosylation reaction can strengthen the entire gel structure and prevent fragmentation. Furthermore, Zha et al. (2019) demonstrated that glycosylation not only improves the functionality of poorly water-soluble plant proteins but also reduces the pronounced beany flavors. Enzymatic hydrolysis and glycosylation have been extensively demonstrated to enhance the functional properties of SPI. However, further exploration is needed to determine whether the combination of these two methods has a synergistic effect on improving the quality of DPY.

Papain is classified as a limited cysteine hydrolase. It can exhibit significant proteolytic activity towards proteins, short-chain peptides, amino acid esters, and amide bonds (Victorino da Silva Amatto et al., 2022). Additionally, the mild enzymatic hydrolysis conditions of papain can effectively avoid the generation of bitterness and reduce the impact on the taste of yogurt. Gum arabic (GA) is a highly branched polysaccharide with acid stability, which can significantly improve the solubility of proteins by glycosylation reactions. In this work, SPI was treated with papain for different enzymatic hydrolysis pretreatment times. Subsequently, SPI enzymatic hydrolysis products were combined with GA through glycosylation reactions. This work aimed to investigate the effect of enzymatic hydrolysis pretreatment combined with glycosylation on the structural and functional properties of SPI, as well as to evaluate the impact on texture and flavor of DPY made by partially replacing the milk protein with glycosylated SPI after enzymatic hydrolysis pretreatment. The findings of this study would provide a theoretical basis for the formulation of emerging yogurt products.

2. Materials and methods

2.1. Materials

Soybean protein isolate (SPI) was obtained from Yuanye Bio-Technology Co., Ltd. (Shanghai, China). Gum acacia (GA) and Papain (200 U/mg) were gained from Macklin Biochemical Technology Co., Ltd. (Shanghai, China). Commercial starter cultures with the product type YO-MIX 300 (*Streptococcus thermophilus and Bacillus bulgaricus*), granulated sugar, and skim milk powder (fat content of 1.3 %, protein content of 34 %) were purchased from the commercial supermarket (Harbin, China). All the other chemicals used analytical grade.

2.2. Pretreatment of SPI with enzymatic hydrolysis

SPI was dissolved in distilled water under continuous stirring for 2 h to obtain SPI solution (4 %, *w/v*) and left it to stand at 4 °C overnight. The pH of the SPI solution was adjusted to 7.0 with NaOH (2 mol/L). Papain (1 %, *w*/w) was added for enzymatic hydrolysis at 55 °C for 0, 10, 20, 30, 40 and 50 min. The process of enzymatic hydrolysis was stopped by heating the mixture to 95 °C for 20 min. SPI enzymatic hydrolysates were obtained and named ESPI0, ESPI10, ESPI20, ESPI30, ESPI40, and ESPI50, respectively.

2.3. Glycosylation of SPI enzymatic hydrolysate

GA (0.8 %,*w/v*) was dissolved in SPI enzymatic hydrolysate under continuous stirring for 1 h. The SPI-GA solution was incubated in a water bath at 95 °C for 2 h and centrifuged at 8000 ×*g* (Eppendorf 5810R, Chennai, India) at 4 °C for 10 min. The supernatant was adjusted to pH 7.0 and freeze-dried for analysis. Finally, the samples were recorded as ESPI0-G, ESPI10-G, ESPI20-G, ESPI30-G, ESPI40-G, and ESPI50-G, respectively. Natural SPI was used as the control and was recorded as NSPI.

2.4. Measurements of the properties of glycosylation of SPI enzymatic hydrolysate

2.4.1. The degree of grafting (DG)

The DG of samples was calculated using the o-phthaldialdehyde (OPA) assay method developed by Chen et al. (2022). The 200 μL sample was mixed with 4 mL of OPA reagent and incubated at 35 °C for 2 min before measuring the absorbance at 340 nm with a Shimadzu UV-1800 spectrophotometer. The control was prepared with water and OPA reagent. The DG was computed according to eq. (1):

$$DG\ (\%) = \frac{A - A_1}{A_1} \times 100\% \quad (1)$$

where A is the free amino group content of SPI, and A_1 is the free amino group content of ESPIs-G.

2.4.2. Solubility

Samples (5 mg/mL) were centrifuged at 10000 ×*g* for 20 min. The solubility was determined by measuring the protein concentration in the supernatant before centrifugation.

2.4.3. Fourier transform infrared spectroscopy (FTIR)

Samples were mixed with KBr and pressed. FTIR spectra were collected using a Spectrum GX infrared spectrometer (PerkinElmer, USA) over the wavenumber range of 4000–400 cm^{-1}, with a resolution of 4 cm^{-1}. The relative content of each secondary structure was determined using the integral area with Peak fit software (version 4.2.0) (Cheng et al., 2024).

2.5. Preparation of the DPY

According to Chen et al. (2023), DPY samples were prepared as follows. Skim milk powder (10 % *w/v*) was mixed with sugar (6 % *w*/w) and reconstituted at 60 °C for 10 min. The mixture was then homogenized at 20/2 MPa pressure (AH-Basic 11, ATS Engineering Inc., Canada) and heated to 90 °C for 30 min. After cooling to 43 °C, glycosylated SPI hydrolysate was added at a ratio of 3:7 (*v*/v) to skim milk (Martin et al., 2016). Commercial starter cultures 2 % (*w*/w) was added to the mixture and incubated in a water bath at 43 °C for 9 h. The prepared yogurt was refrigerated for one day before analysis. The final samples were recorded as DPY0, DPY10, DPY20, DPY30, DPY40 and DPY50, respectively. Traditional yogurt without SPI partially replacing milk protein was set as the control group, recorded as Y. The preparation for

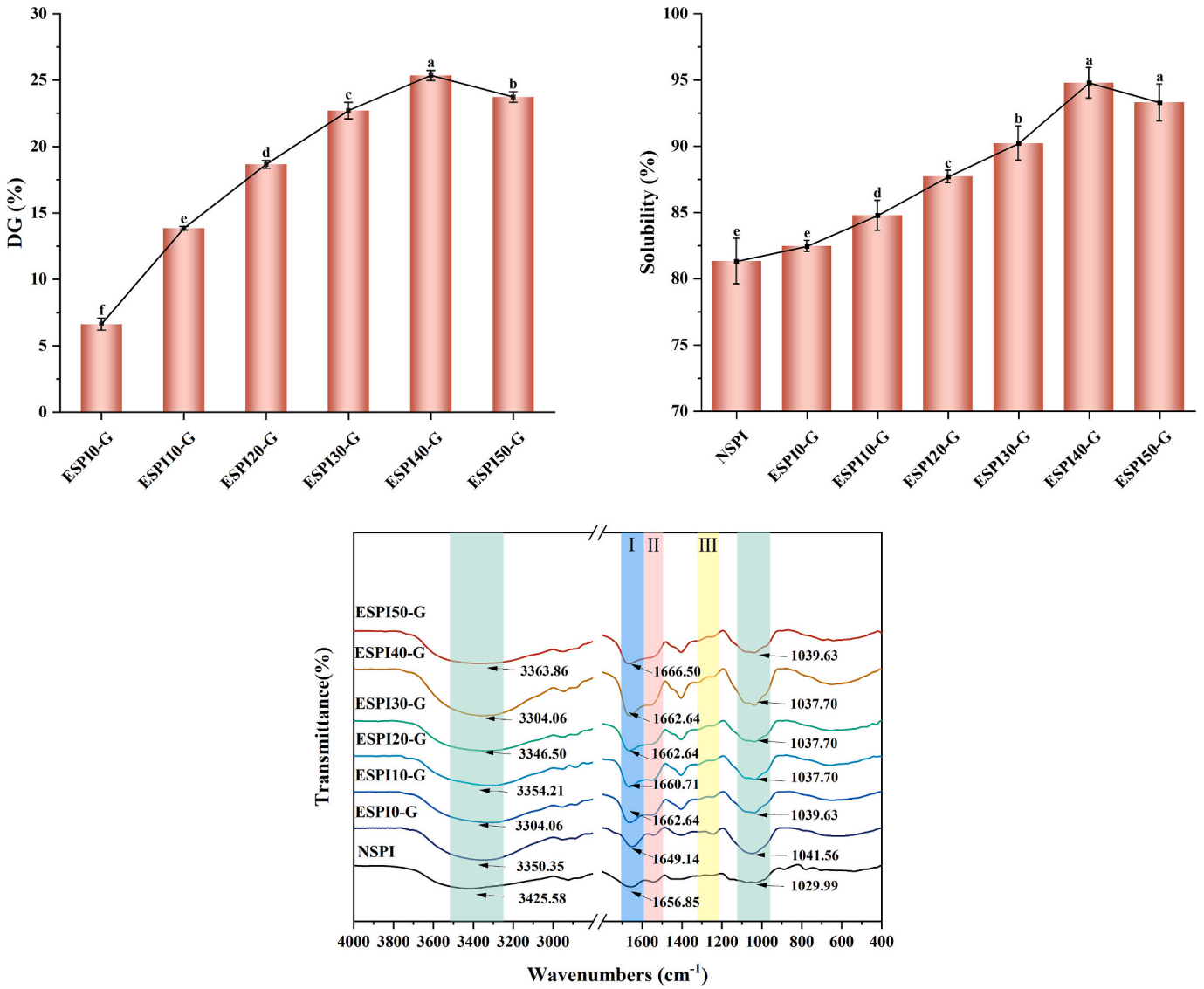

Fig. 1. Degree of grafting (DG) (a), Solubility (b), and Fourier transform infrared spectroscopy (FTIR) (c) of glycosylated SPI treated with different enzymatic hydrolysis times.
Note: The varying lowercase letters represent statistically significant differences ($p < 0.05$) in glycosylated SPI treated with different enzymatic hydrolysis times.

the control group was the same as described above.

2.6. Measurements of the properties of DPY

2.6.1. Macroscopic and microscopic images

Macroscopic and microscopic images were captured using cameras and confocal laser scanning microscopy (CLSM). Approximately 1 mL of yogurt was sampled and stained with Rhodamine B (0.1 % *w/v*), with excitation and emission wavelengths of 543–625 nm, for protein analysis. CLSM (FV3000, OLYMPUS, Japan) captured images at 20-fold magnification with a resolution of 1024 × 1024 pixels.

2.6.2. pH and Titratable acidity (TA)

The pH of the yogurt was determined using a digital pH meter (PHS-3TC, Shanghai Precision Instrument Co., Ltd., China). Diluted yogurt samples (0.5 %, *v*/v) were used to determine titratable acidity (TA) following the method by Xu et al. (2022). In brief, diluted yogurt samples were used to determine TA content according to GB 5009.239–2016. A phenolphthalein solution (2 mL, 5 % *w/v*) was added to the diluted samples as an indicator. The mixture was titrated with 0.1 M NaOH to express pink and did not fade within 30 s. TA (°T) was calculated as the volume of NaOH consumed (mL) multiplied by ten.

2.6.3. Particle distribution and Zeta potential

Zeta potential and particle size distribution of yogurt diluted 50 times were measured using a Zetasizer Nano-ZS90 (Malvern Instruments Ltd., Great Malvern, UK). The refractive indices of the particle and dispersant were established as 1.75 and 1.33, respectively.

2.6.4. Texture

Textural analysis was performed using a texture analyzer (TA-XT Plus, Stable MicroSystems Ltd., UK). Measuring parameters: speed before measurement 1.0 mm/s; test speed 1.0 mm/s; The measured velocity is 1.0 mm/s; The pressing distance is 10 mm; Load type Auto-10 g; A/BE-d35 probe; Data acquisition rate: 200 pps. These indicators included hardness, adhesion, consistency, and cohesion.

2.6.5. Water holding capacity (WHC) and Syneresis

The WHC and syneresis of yogurt samples were assessed after centrifugation at 1000 ×*g* at 4 °C for 20 min. The WHC was determined

using eqs. (2) and (3):

$$WHC\ (\%) = \frac{W - W_1}{W} \times 100\% \quad (2)$$

$$Syneresis\ (\%) = \frac{W_1}{W} \times 100\% \quad (3)$$

where W is the weight of yogurt before centrifugation, and W_1 is the weight of the supernatant after centrifugation of yogurt.

2.6.6. Rheological properties

The rheological properties of the yogurt were assessed using a rheometer (R/S, Brookfield Instruments Co., Ltd., Stoughton, MA) equipped with a vane spindle (*V*-20/40). Apparent viscosity, oscillation frequency sweep, and creep recovery test were performed. The apparent viscosity was measured over a range of shear rates from 0.1 to 100 s^{-1}, while the oscillation frequency sweep was conducted from 0.1 to 10 rad/s. Creep recovery was evaluated by constant stress of 1 Pa (within the linear viscoelastic region) for 120 s. Subsequently, the stress was instantly removed to monitor recovery within 240 s.

2.6.7. Volatile compounds

Solid-phase microextraction (SPME) process: SPME/GC–MS was employed to extract and analyze the volatile compounds present in yogurt according to the method of Xu et al. (2022). 7 mL of samples were supplemented with 20 μL of *2-Methyl-3-heptanone* (250 μg/mL) as the internal standard, and subsequently transferred to a headspace vial. After equilibrating at 60 °C for 15 min, the SPME fiber (CTC Analytics AG, Zwingen, Switzerland) was subsequently introduced into the headspace vial for extraction at 60 °C for 30 min and then transferred to the injection port of the GC system.

GC–MS analysis was conducted using a TSQ 1310 gas chromatograph coupled with a TSQ 9000 triple quadrupole mass spectrometer (Thermo Scientific, Shanghai, China). The GC oven temperature program started at 45 °C for 3 min, increased to 100 °C at 6 °C/min, reached 230 °C at 10 °C/min, and was held for 7 min. The MS conditions used an electron impact ionization mode with an electron energy of 70 eV and ion source temperature of 250 °C. The mass spectrometer scan range covered *m/z* values ranging from 33 to 350.

2.7. Statistical analysis

The experiments were conducted in triplicate, and the results were presented as mean ± standard deviation. This study was conducted using SPSS version 22.0 software, Origin 2021 software for graphing, and $p < 0.05$ as the significance level.

3. Results and discussion

3.1. The character of composite solution

3.1.1. Degree of grafting (DG)

The changes in the free amino content of SPI can serve as an indicator of the degree of interaction between proteins and polysaccharides, further evaluating the degree of glycosylation between SPI and GA at different enzymatic pretreatment times (Dai et al., 2023). As shown in Fig. 1a, the DG of ESPIs-G increased from 6.62 % to 25.36 % as the enzymatic hydrolysis pretreatment time increased from 0 to 40 min. This is likely because the carboxyl terminus of arginine and lysine in SPI was cleaved precisely by papain, opening the spheroid structure of SPI, and exposing more free amino groups (Kong et al., 2008). With the increase in enzymatic hydrolysis pretreatment time, an increased number of binding sites between SPI and GA became exposed. Consequently, a greater amount of GA can interact with SPI via hydroxyl groups present on the polysaccharide chains, resulting in an elevated DG. The results of DG showed a decreasing trend when the enzymatic hydrolysis time increased to 40 min. This may be because prolonged enzymatic hydrolysis led to the re-transfer of some of the lysine residues exposed on the surface of SPI to a more hydrophobic environment. This alteration hindered the ability of the $-NH_2$ groups to conjugate with GA (Zhang et al., 2023). This reduced the binding capacity between SPI and GA, leading to a decrease in DG. Overall, appropriate enzymatic hydrolysis pretreatment can enhance the degree of SPI glycosylation.

Table 1
The secondary structure of glycosylated SPI treated with different enzymatic hydrolysis times.

Samples	Secondary structure composition (%)			
	α-helix	β-sheet	β-turn	Random coil
SPI	30.09 ± 1.55^{bc}	19.61 ± 1.04^{d}	21.03 ± 1.05^{c}	29.28 ± 0.80^{a}
ESPI0-G	38.04 ± 0.64^{a}	19.98 ± 1.19^{d}	21.93 ± 0.33^{c}	20.05 ± 0.37^{d}
ESPI10-G	31.14 ± 0.26^{b}	21.07 ± 0.77^{d}	25.53 ± 0.24^{a}	22.26 ± 0.23^{c}
ESPI20-G	28.99 ± 0.32^{c}	22.98 ± 0.45^{c}	24.58 ± 0.62^{ab}	23.44 ± 1.02^{b}
ESPI30-G	30.82 ± 0.78^{b}	24.95 ± 0.29^{b}	23.62 ± 1.38^{b}	20.62 ± 0.44^{d}
ESPI40-G	34.92 ± 0.63^{b}	27.40 ± 0.83^{a}	20.68 ± 0.59^{c}	17.00 ± 0.35^{e}
ESPI50-G	35.90 ± 0.19^{b}	28.19 ± 0.95^{a}	21.80 ± 0.58^{c}	14.11 ± 0.44^{f}

Values are given as the mean values from triplicate measurements. Significant differences ($p < 0.05$) between means in the same column are indicated by distinct lowercase letters.

3.1.2. Solubility

The solubility of SPI is a critical factor in improving gel properties and is affected by the DG of SPI (Wang et al., 2023). The increased solubility of SPI contributed to a reduction in rigidity and an improvement in compatibility with other proteins, thereby resulting in improved syneresis of the gel. The solubility results of enzymatic hydrolysis pretreatment combined with glycosylation of SPI are shown in Fig. 1b. The solubility of ESPIs-G was significantly increased ($p < 0.05$) compared to NSPI, especially ESPI40-G (94.77 %). On the one hand, GA increased hydrophilic groups, making SPI more hydrophilic. On the other hand, the complex multi-branched structure of GA contributed to the repulsive effect between protein molecules and enhanced the dispersion stability of SPI in aqueous solution (Parandi et al., 2024). Additionally, enzymatic hydrolysis pretreatment enhanced the glycosylation degree of SPI, facilitating the incorporation of hydroxyl groups from GA into the SPI structure. This modification accounts for the increased solubility of SPI.

3.1.3. Fourier transform infrared spectroscopy (FTIR)

Fig. 1c represents the FTIR of SPI and different samples by enzymatic hydrolysis pretreatment combined with glycosylated SPI. Amide *I* (1600–1700 cm^{-1}) is mainly used for protein conformation analysis. Compared to NSPI, the absorption band of ESPIs-G shifted to different degrees, indicating that enzymatic hydrolysis pretreatment combined with glycosylation altered the secondary structure of SPI. Furthermore, the increase in absorption band intensity was observed at 3000–3700 cm^{-1} and 900–1200 cm^{-1}, indicating the increase of hydroxyl groups in SPI by enzymatic hydrolysis pretreatment at different times combined with glycosylation, causing the stretching vibration of O—H (Liu et al., 2018). This confirmed that GA has been successfully grafted onto SPI. Meanwhile, the absorption band observed at 900–1200 cm^{-1} is the characteristic absorption band of polysaccharide. It is attributed to the significant increase in newly formed C—N covalent bonds during the glycation reaction between SPI and GA (Sun et al., 2020). The observed increase in the number of hydroxyl groups, along with the enhancement of polysaccharide characteristic bands, suggested a greater extent of GA grafting onto SPI. This finding further substantiates that enzymatic hydrolysis pretreatment facilitates the glycosylation of SPI.

The relationship between the secondary structures and band wavenumbers was determined through Gaussian peak fitting of the amide I band in FTIR spectroscopy. As shown in Table 1, compared to NSPI, the α-helix content of ESPI0-G was significantly increased, and the random coil content was significantly decreased ($p < 0.05$). This phenomenon

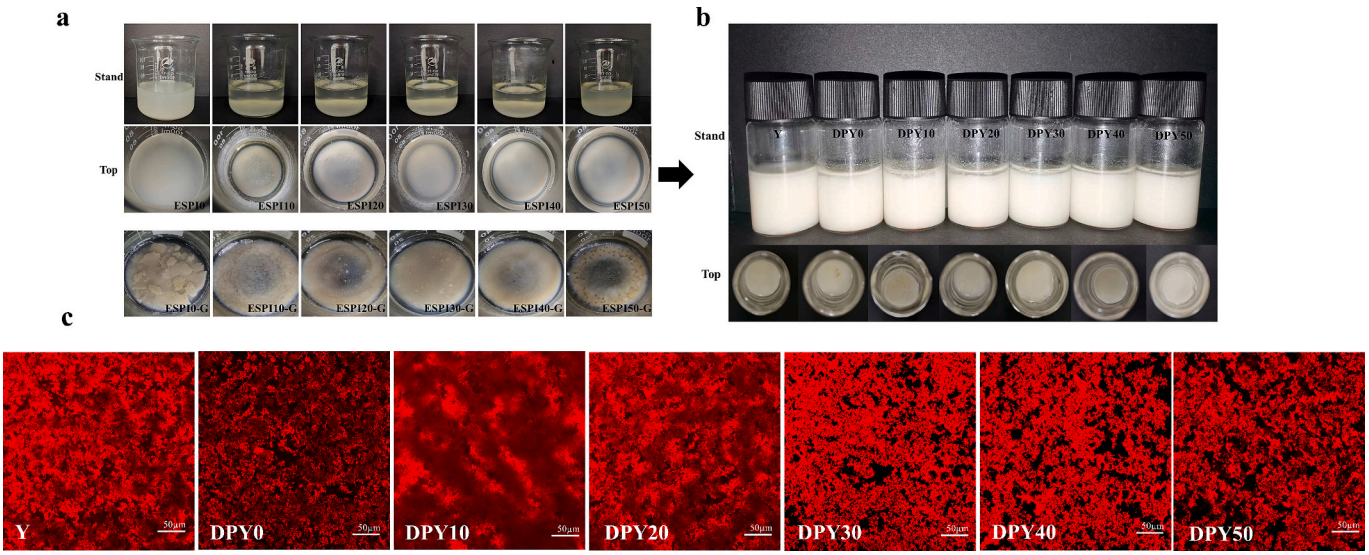

Fig. 2. The macroscopic images of glycosylated SPI with enzymatic hydrolysis pretreatment at different times (a), macroscopic images (b) and microscopic images (c) of dual-protein yogurt prepared by glycosylated SPI treated with different enzymatic hydrolysis times.
Note: The protein network is highlighted in red, with Rhodamine B used to stain the proteins. Meanwhile, the dark areas represent the water phase and syneresis. (For interpretation of the references to colour in this figure legend, the reader is referred to the web version of this article.)

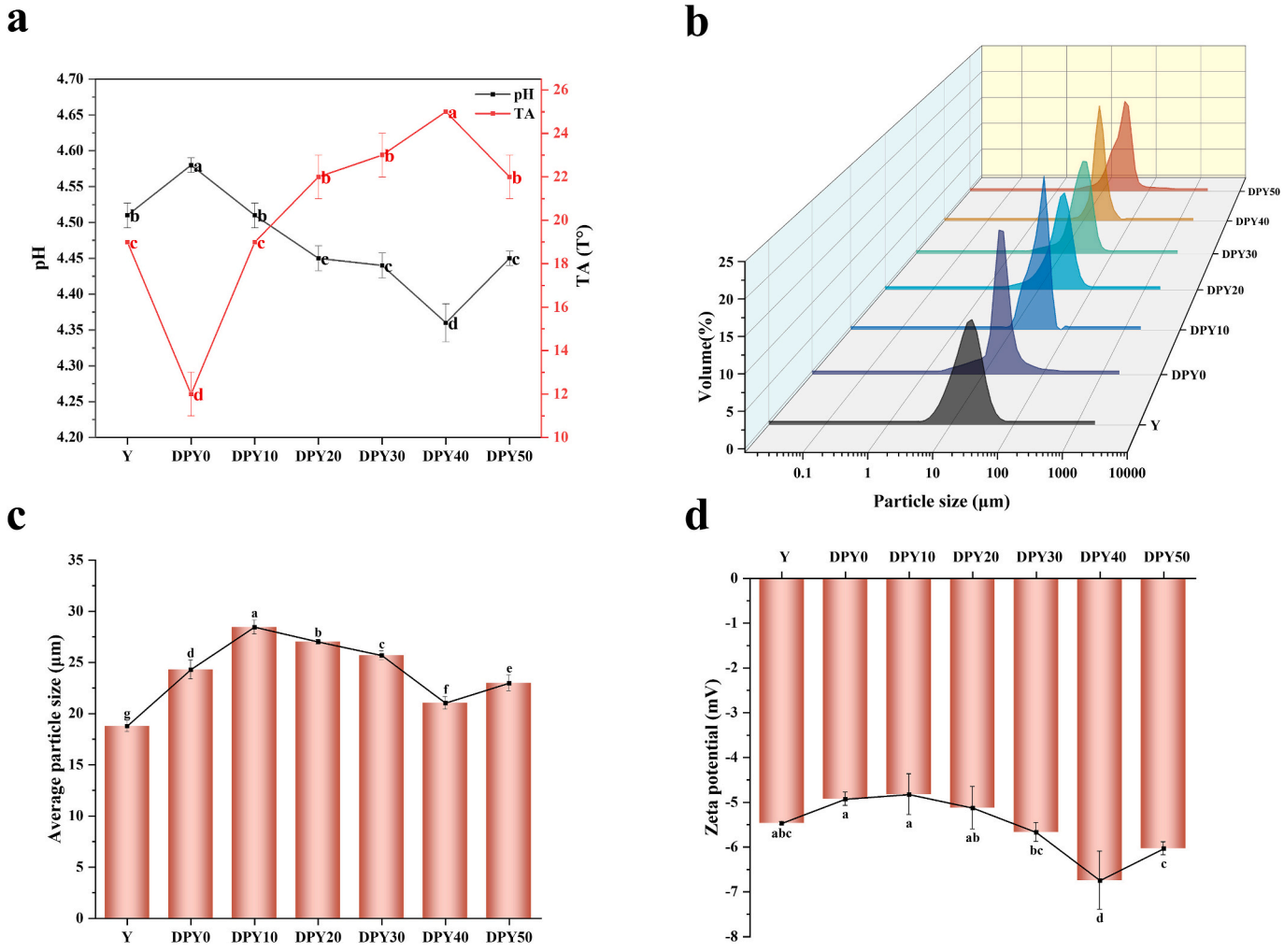

Fig. 3. The pH and Titratable acidity (TA) (a), Particle size distribution (b), average particle size (c), and Zeta potential (d) of dual-protein yogurt prepared by glycosylated SPI treated with different enzymatic hydrolysis times.
Note: The varying lowercase letters represent statistically significant differences in different samples ($p < 0.05$).

can be attributed to the SPI having an open structure after enzymatic hydrolysis, which facilitated the formation of additional hydrogen bonds with GA, thereby stabilizing its spatial conformation. The protein structure began to shift from disordered to ordered. With the increase in enzymatic hydrolysis pretreatment time, the α-helix and β-sheet contents showed a trend of declining and then increasing. The decrease in α-helix and β-sheet content may be due to enzymatic hydrolysis disrupting hydrogen bonding in the SPI molecular chain, indicating the loss of ordered secondary structures and the formation of more flexible structures for SPI (Zhong et al., 2019). Additionally, Zhao et al. (2023) have reported that the absence of voids in the compact α-helix structure was not conducive to the gel properties of proteins, whereas the conformational stability and compactness of β-sheet were inferior to those of α-helix. Therefore, the increase of β-type structures in SPI from enzymatic pretreatment combined with glycosylation may be beneficial to increase the molecular flexibility of SPI and thus improve the gel properties of SPI.

3.2. The character of yogurt quality

3.2.1. Macroscopic and microscopic images

The gel texture of DPY is primarily determined by the pre-yogurt formation state of the protein solution. The glycosylated SPI solution obtained by enzymatic hydrolysis pretreatment at different times and the DPY prepared by partially replacing milk protein with them are shown in Fig. 2a and b. As shown in Fig. 2a, ESPI0-G had a hard and fragile protein cluster, which may cause the protein to form a rigid and fragile gel following acid coagulation. This condition was not conducive to the formation of a desirable texture for DPY. This demonstrated that glycosylation modification of SPI has a weak effect on improving the gel texture of DPY. With the increase in enzymatic hydrolysis pretreatment time, the phenomenon of protein aggregation in glycosylated SPI solution was mitigated. Especially, ESPI40-G showed a delicate and uniform state after 40 min of enzymatic hydrolysis pretreatment. This may be attributed to the enzymatic hydrolysis pretreatment increasing the DG of SPI, introducing more hydroxyl groups, and enhancing the solubility of SPI. However, the prolonged enzymatic hydrolysis pretreatment resulted in the formation of brown clumps. Briefly, appropriate enzymatic hydrolysis pretreatment combined with glycosylation is conducive to improving the solubility of SPI, which may reduce the rigid structure of the gel and improve the formation of the gel texture of DPY.

We partially replaced milk protein with ESPIs-G to prepare DPY. Fig. 2b revealed that Y and DPY had significantly different appearances, syneresis degrees, and textures. In our previous experiment, the yogurt prepared with NSPI as raw material failed to coagulate, so we will not discuss it subsequently. From Fig. 2c, Y exhibited a compact and high-connectivity protein network with fewer void areas. The microstructure of Y consisted of numerous small pores formed through the interactions among clusters and chains of casein. Other studies have reported a similar structure for yogurt (Alkobeisi et al., 2022). The protein network in DPY0 prepared by glycosylated SPI without enzymatic hydrolysis exhibited increased density and hardness. This may be attributed to the reaggregation of hard ESPI0-G during the heating process, which is consistent with the results observed in Fig. 2a. The dense and hard network structure of DPY gradually disintegrated as the enzymatic hydrolysis pretreatment time increased. After 30 min of enzymatic hydrolysis, a highly connected protein network structure gradually formed in DPY. Meanwhile, the large aggregated protein particles of ESPIs-G were disintegrated as the enzymatic hydrolysis pretreatment time increased, leading to a decrease in rigid structure and an increase in solubility. This may be because SPI with high DG was accompanied by a high viscosity, which increased the compatibility between SPI and milk protein. The increased compatibility facilitated the network cross-linking between SPI and milk protein, which made it easier for SPI and milk protein to form a compact protein network structure. Therefore, the DPY prepared from them was similar to traditional yogurt in appearance.

Table 2
The texture property in dual-protein yogurt prepared by glycosylated SPI treated with different enzymatic hydrolysis times.

Parameters	Hardness (g)	Adhesion (g.s)	Consistency (g.s)	Cohesion (g)
Y	111.11 ± 2.80^{a}	−286.05 ± 5.60^{g}	1095.34 ± 8.65^{a}	−29.05 ± 0.37^{g}
DPY0	86.72 ± 3.83^{d}	−146.67 ± 1.79^{d}	859.89 ± 48.26^{cd}	−22.28 ± 1.40^{e}
DPY10	84.06 ± 3.09^{d}	−63.74 ± 2.75^{a}	766.57 ± 69.65^{d}	−10.18 ± 1.48^{a}
DPY20	85.26 ± 3.17^{d}	−100.43 ± 0.79^{b}	808.60 ± 97.59^{cd}	−13.10 ± 0.16^{b}
DPY30	101.97 ± 1.98^{b}	−131.98 ± 2.18^{c}	935.77 ± 62.11^{bc}	−17.03 ± 0.11^{c}
DPY40	113.51 ± 3.11^{a}	−178.78 ± 7.76^{f}	1056.22 ± 129.91^{ab}	−25.53 ± 0.60^{f}
DPY50	95.08 ± 1.32^{c}	−163.45 ± 2.30^{e}	891.73 ± 61.03^{cd}	−20.76 ± 0.27^{d}

Values are given as the mean values from triplicate measurements. Significant differences ($p < 0.05$) between means in the same column are indicated by distinct lowercase letters.

3.2.2. pH and Titratable acidity (TA)

The lactic acid bacteria can facilitate the acidic coagulation of proteins by producing lactic acid, which affects the DPY gel degree (Zang et al., 2023). Therefore, the pH and TA of DPY were shown in Fig. 3a, the TA value of DPY0 (12°T) was lower than Y (19°T). The utilization ability of acid-producing microorganisms in milk protein was higher than SPI, resulting in a lower TA in DPY0. As the enzymatic hydrolysis pretreatment time increased, the TA of DPY exhibited an initial upward trend followed by a subsequent decline, reaching its peak value of 25°T at DPY40. Additionally, the nitrogen sources required for lactobacillus fermentation in yogurt mainly consist of free amino acids, such as hydroxyproline, aspartic acid, proline, and serine, along with small-molecule proteins (Prasad et al., 2022). After enzymatic hydrolysis pretreatment, ESPIs-G introduced more GA with high DG to the system. This made more carbon sources available, which increased the production of lactic acid and improved the TA in DPY.

3.2.3. Particle distribution and Zeta potential

The distribution and size of DPY particles significantly influence their structural integrity, sensory properties, and overall stability. Generally, a narrower particle size distribution and smaller particles result in a more stable yogurt gel structure and more refined sensory properties (Mehta et al., 2023). As shown in Fig. 3b and c, the particle size peak of DPY shifted to the right and became narrower. Additionally, the average particle size increased from 18.77 ± 1.53 μm to 26.15 ± 1.59 μm compared to Y. This could be attributed to the SPI having a higher particle size than milk protein, resulting in a larger particle size in DPY. As the enzymatic hydrolysis pretreatment time increased, the average particle size of DPY showed a decreasing trend, followed by an increase. Additionally, there was a narrowest peak width and a minimum average particle size in the DPY40 (20.69 ± 2.12 μm). These findings suggested that DPY40 has similar stability to Y. This can be attributed to the appropriate enzymatic hydrolysis pretreatment combined with glycosylation opening up the SPI structure. The introduction of multi-branched GA via the glycosylation reaction also contributed to the spatial stability of SPI. This may be attributed to the presence of GA with a multi-branched structure between proteins, which reduced protein aggregation and thus lowered the average particle size of DPY. The narrower peak width and smaller average particle size of DPY may have a more delicate taste. This further showed that glycosylation after 40 min of SPI enzymatic hydrolysis is beneficial for improving the sensory qualities of DPY.

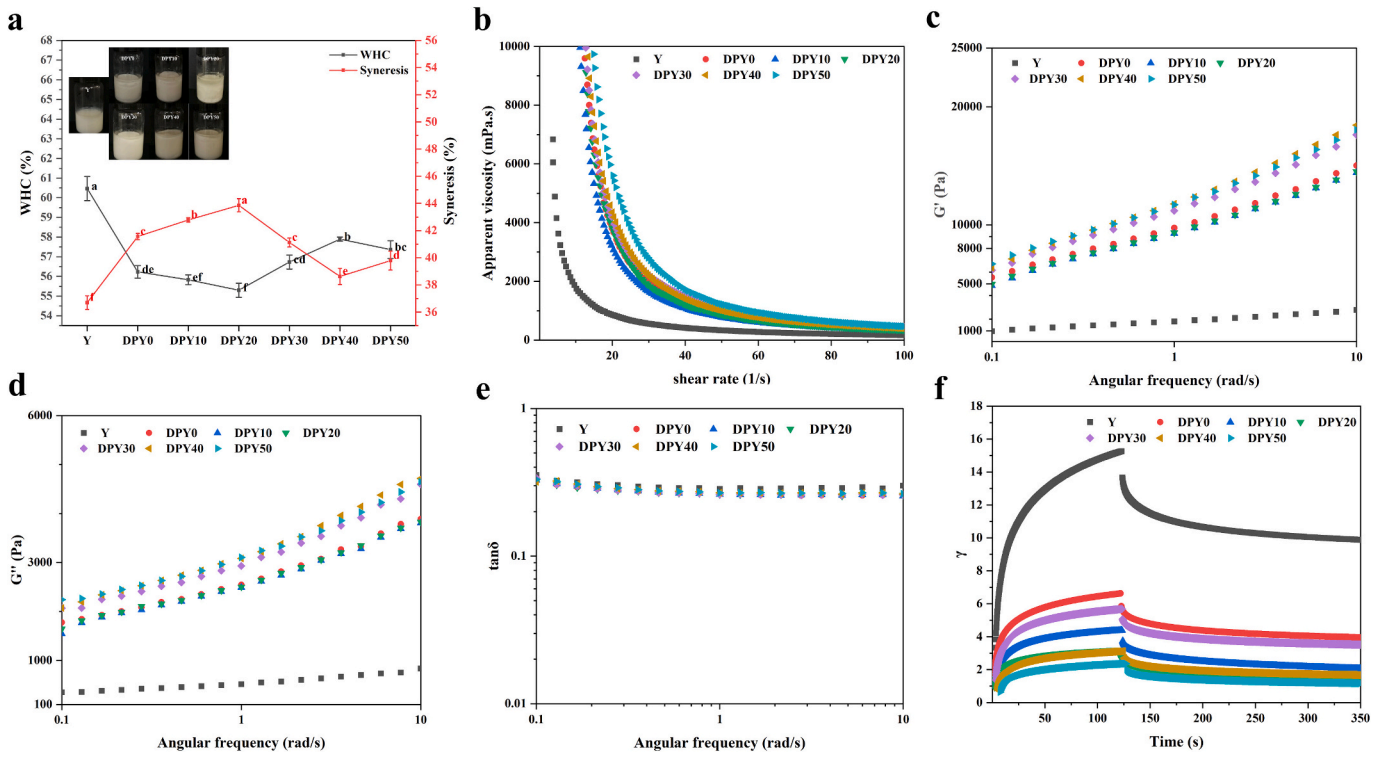

Fig. 4. Water holding capacity (WHC) and Syneresis (a), Apparent viscosity (b), Oscillation frequency sweep curves (c-e), and Creep recovery curves (f) of dual-protein yogurt prepared by glycosylated SPI treated with different enzymatic hydrolysis times.
Note: The varying lowercase letters represent statistically significant differences in different yogurt ($p < 0.05$).

The stability of the gel system in SPI and milk protein is influenced by the absolute zeta potential. Based on previous studies, the electrostatic interactions of proteins are positively correlated with the stability of the yogurt system (Shen et al., 2018). The zeta potential of yogurt prepared by different ESPIs-G is shown in Fig. 3d. As the enzymatic hydrolysis pretreatment time increased, the potential values of DPY first rose and then fell, peaking at DPY40. In the first 40 min of enzymatic hydrolysis pretreatment, the absolute value of the potential in DPY increased. This is because more polar groups were exposed on the SPI surface, raising the electrical potential (Li et al., 2021). Furthermore, the protein complex formed by the SPI and milk protein carried more isotypic charges on its surface, which increased the electrostatic repulsion and improved the potential values. The stability of the gel system was also greatly enhanced in DPY.

3.2.4. Texture

The texture properties of DPY are influenced by the microstructure. A protein network structure with higher density and connectivity may lead to a stronger and more structured gel (Muncan et al., 2020), thereby exerting a positive influence on the quality of DPY and potentially impacting WHC. The hardness, adhesion, consistency, and cohesion of DPY are presented in Table 2. The hardness, adhesion, consistency, and cohesion of DPY0 exhibited a significant decrease compared to Y ($p < 0.05$). This could potentially be attributed to the steric hindrance caused by ESPIs-G, which disrupted the cross-linking of milk proteins and led to the formation of a weak protein network structure (Wang, et al., 2023). Consequently, the compromised resistance of yogurt to external forces led to a reduction in its hardness. With the increase in enzymatic hydrolysis pretreatment time, the hardness, adhesion, consistency, and cohesion of DPY showed an overall trend of first increasing and then decreasing. Compared to DPY0, the hardness, adhesion, consistency, and cohesion of DPY40 exhibited significant improvements of 30.89 %, 21.89 %, 22.83 %, and 14.57 %, respectively. These findings suggested that appropriate enzymatic hydrolysis pretreatment improved the effect of glycosylation on the texture properties of DPY. This was consistent with the observation of microstructure, indicating that a compact protein network structure was more conducive to forming the hard and thick texture of yogurt. A similar study showed that the intensive network structure of proteins enhanced the viscosity of the yogurt (Wei et al., 2023). Additionally, the hardness and consistency of DPY40 were not significantly different from Y ($p > 0.05$), indicating that they may have similar gel network structure and WHC.

3.2.5. Water holding capacity (WHC) and Syneresis

The WHC of yogurt is influenced by its texture properties, which can subsequently affect the overall quality and taste of yogurt (Yang et al., 2022). From Fig. 4a, a negative correlation between the WHC and syneresis of yogurt. This agreed with a study by El-Kholy et al. (2019). Compared to Y, DPY had a lower WHC and higher syneresis. As the enzymatic hydrolysis pretreatment time increases, the WHC of DPY showed an initial increase followed by a decrease, while syneresis was the opposite. Compared to DPY0, the syneresis of DPY40 was reduced by 7.61 % to reach 38.63 %. Meanwhile, the WHC of DPY40 increased to 57.90 %. This indicated that appropriate enzymatic hydrolysis pretreatment combined with glycosylation can effectively improve the WHC of DPY. This phenomenon can also be observed in Fig. 2b. The WHC of DPY was far lower than Y, which may be related to the unstable gel network structure of DPY. The unstable gel network was formed due to the incompatibility between milk protein and SPI, leading to reduced hardness and adhesion (Wang et al., 2023). After 30 min of enzymatic hydrolysis pretreatment, the WHC of DPY was significantly improved and showed a higher WHC at 40 min. This is due to the increased solubility of glycosylated SPI after enzymatic hydrolysis for 40 min, thereby enhancing the compatibility between SPI and milk protein. Consequently, the formation of a dense and highly interconnected gel network structure led to an improved WHC in DPY40. The increased hardness, adhesion, consistency, and cohesion of DPY40 contribute to its enhanced water binding capacity, resulting in higher WHC and lower

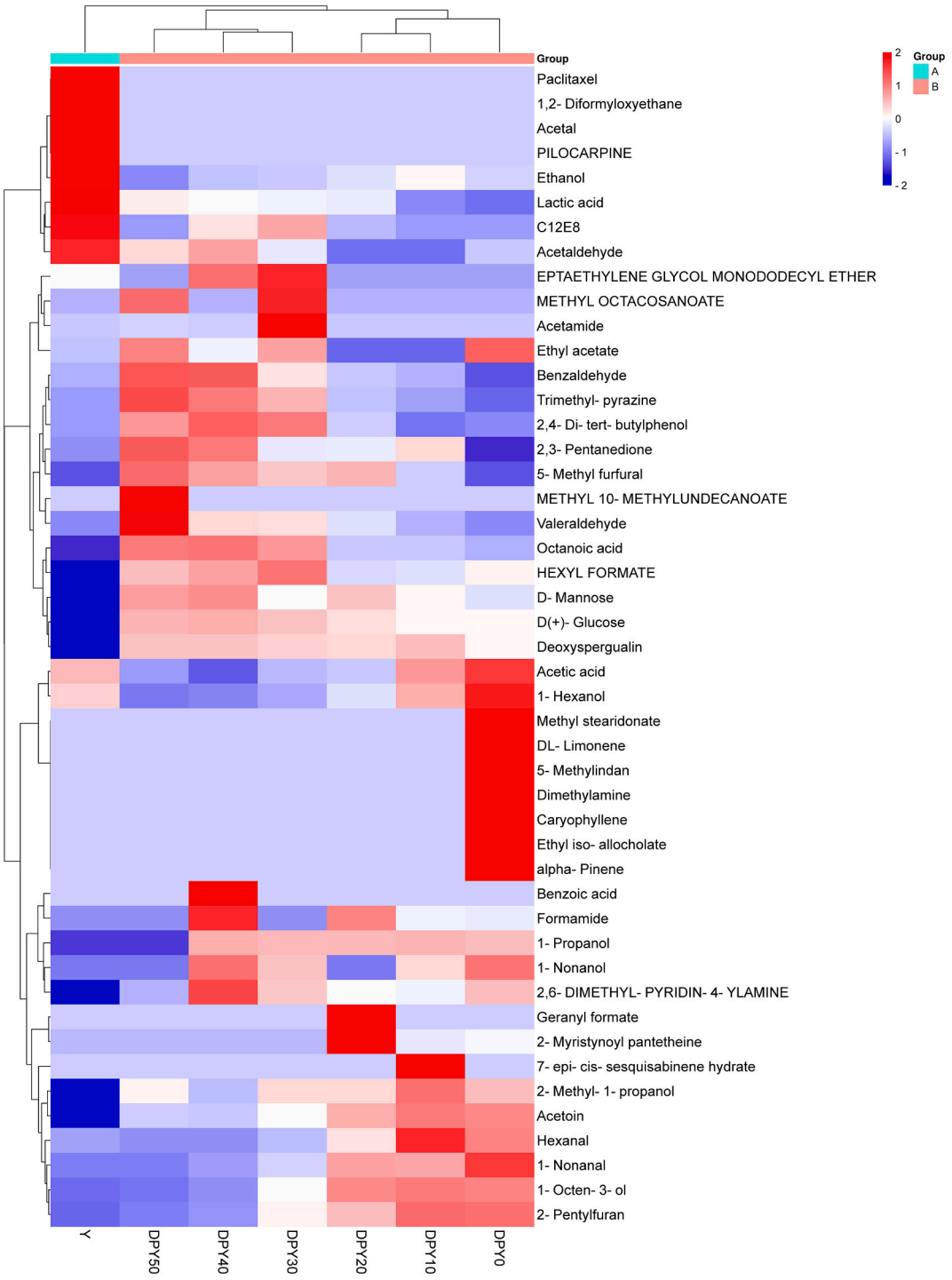

Fig. 5. The flavor of dual-protein yogurt prepared by glycosylated SPI treated with different enzymatic hydrolysis times.

syneresis (Metry & Owayss, 2009). Moreover, the strong electrostatic interaction between ESPI40-G and milk protein in DPY40 was conducive to the stability of the gel structure. The WHC of yogurt and observed particle size/zeta potential, hardness, microstructure, etc. were well confirmed.

3.2.6. *Rheological properties*

The apparent viscosity, oscillating frequency sweep, and creep recovery tests of DPY were studied to characterize the effects of ESPIs-G on the viscoelasticity and overall quality of the gel in DPY. Higher viscoelasticity is beneficial for the stability of DPY and even affects flavor retention.

The texture of yogurt was determined by its apparent viscosity to some extent. From Fig. 4b, all yogurts presented a clear pseudoplasticity behavior. Additionally, the apparent viscosity of DPY was higher than Y. As the enzymatic hydrolysis pretreatment time increased, the apparent viscosity of DPY decreased and then increased. All yogurts exhibited shear thinning behavior as a result of the applied shear force that disrupted the casein chain and caused weakness in the electrostatic and hydrophobic connections within the yogurt network (Alkobeisi et al., 2022). However, the apparent viscosity of DPY showed an opposite trend to the adhesion of its texture properties. This might be attributed

Table 3
The content of compounds with beany flavor and bitterness in dual-protein yogurt prepared by glycosylated SPI treated with different enzymatic hydrolysis times.

Compounds		Relative peak area (μg / kg)						
		Y	DPY0	DPY10	DPY20	DPY30	DPY40	DPY50
Beany flavor	1-Hexanol	8.87	18.00	10.65	5.20	2.45	0.44	0
	1-Octen-3-ol	0.74	10.78	11.04	10.56	6.33	2.12	1.07
	Ethyl acetate	0.33	1.06	0	0	0.83	0.48	0.94
	Hexanal	70.33	156.01	194.34	118.30	82.15	62.35	64.00
	1-Nonanal	9.55	5.69	5.63	6.34	8.67	11.01	11.19
	2-Pentylfuran	0	2.07	1.34	1.37	0.54	0.22	0
	Benzaldehyde	2.78	26.76	27.40	20.66	16.25	6.60	5.08
	Total	92.60	220.37	250.40	162.43	117.22	83.22	82.28
Bitter	2-Methyl-1-propanol	0	1.40	1.73	1.28	1.28	0.83	1.17
	Benzaldehyde	2.55	1.69	2.63	2.84	3.67	5.01	5.90
	Valeraldehyde	0	0	0.14	0.29	0.50	0.52	1.21
	5-Methyl furfural	0	0	1.31	2.73	2.45	2.89	3.53
	Total	2.55	3.09	5.81	7.14	7.90	9.25	11.01

to the fact that the spherical structure of SPI made it harder than milk protein and gave it a stronger resistance to external stress. The apparent viscosity of DPY increased with the increase of enzymatic hydrolysis pretreatment time, which may be related to the production of acid (Wang et al., 2022). The increase of TA in DPY promoted the formation of gel with a viscous texture between milk protein and SPI. The enzymatic hydrolysis pretreatment facilitated increased glycosylation of SPI, introducing more GA to SPI and subsequently enhancing the apparent viscosity of DPY.

The oscillation frequency sweep expresses the elasticity and viscosity of the DPY gel as the storage modulus (G′) and loss modulus (G″), respectively. As shown in Fig. 4c and d, all yogurts exhibited viscoelastic characteristics with G′ higher than G″. Both G′ and G″ exhibited frequency dependence, which gradually increased with increasing frequency. In contrast to Y, DPY exhibited elevated G′ and G″ values, as well as a more pronounced frequency dependence on G′ and G″, suggesting a potential weakness in the crosslinking effect of the gel. Pang et al. (2020) reported that the degree of crosslinking did not always correlate with gel strength. A less dense network with a medium degree of connectivity can hold more water, resulting in a stronger gel. This was consistent with the results of WHC. The frequency induction behavior of DPY was also affected by enzymatic hydrolysis pretreatment at different times combined with glycosylation of SPI. The G′ and G″ of DPY prepared by enzymatic hydrolysis pretreatment of SPI for 30–50 min were higher than 0–20 min. This suggested that the combination of appropriate enzymatic hydrolysis pretreatment and glycosylation of SPI was beneficial for improving the viscoelasticity of DPY. Fig. 4e shows the corresponding tan δ (G"/G′) values under frequency scanning conditions. Generally, the larger tan δ, the more viscous/fluid behavior of the sample. The tan δ values are between 0.1 and 1, which is typical of weak gel systems. This was consistent with the rheological properties of yogurt described by Xu et al. (2022).

Creep recovery is related to microstructural changes and reorientation of chemical bonds (Lei et al., 2021), which is used to characterize the viscoelasticity of yogurt. The viscoelasticity of yogurt can be determined by examining the slope of the curve after the force is removed. A flatter curve, indicating a smaller slope, indicates a higher viscoelasticity of yogurt (Fan et al., 2022). From Fig. 4f, the Y obtained the highest deformation, followed by the DPY. Additionally, the DPY recovered to the lowest plateau of deformation in a relatively short time as the enzymatic hydrolysis pretreatment time increased. While the Y was still in a period of decline, indicating a higher proportion of viscous deformation in the Y. This indicated that the inclusion of ESPIs-G promoted the formation of a network structure with greater elasticity, hence increasing the structural integrity to withstand external stress.

3.2.7. Flavor

The GC–MS spectrum of DPY prepared by adding ESPIs-G is shown in Fig. 5. A total of 47 volatile compounds, including ten esters, seven alcohols, seven aldehydes, five alkenes, four acids, two ketones, one phenol, etc., were identified. Among them, 1-hexanol, 1-octen-3-ol, ethyl acetate, hexanal, 1-nonanal, 2-pentylfuran, and benzaldehyde were shown in grassy, leafy, mushroomy, and rancid flavors, which were typical flavor compounds with the beany flavor. Furthermore, 2-methyl-1-propanol, benzaldehyde, valeraldehyde, and 5-methyl furfural were typical flavor compounds with the bitter. The DPY produced by ESPIs-G exhibited a reduction in beany flavor compared to Y. However, as the enzymatic hydrolysis proceeded, there was a slight increase in bitter compounds (as shown in Table 3). Nevertheless, this increase had a minimal effect on the bitterness threshold or taste. This suggested that the DPY prepared by ESPIs-G will not negatively impact the flavor of yogurt and may potentially enhance the flavor profile. This is because the beany flavor mainly comes from lipid oxidation and protein degradation. The degradation of SPI was facilitated by papain, reducing the retention rate of the compounds with the beany flavor. Bitterness in protein hydrolysates is typically linked to peptides with hydrophobic amino acids (Liu et al., 2022). Due to the mild enzymatic hydrolysis of papain, the hydrolysates were mostly macromolecular peptides with the α-helix or irregular curl structure of enzymatic hydrolysis pretreatment. The hydrophobic groups within these peptides were sequestered within the protein molecules, hindering their interaction with taste receptors on the taste buds and thereby mitigating the perception of bitterness. Additionally, the peptides and free amino acids produced by enzymatic hydrolysis increased the substrate of the glycosylated SPI, thereby improving the aroma and flavor of glycosylation products.

4. Conclusion

This study showed that glycosylated SPI after enzymatic hydrolysis pretreatment at different times was successfully applied in yogurt to partially substitute milk protein. GA was successfully grafted onto SPI hydrolysate and verified by DG. Enzymatic hydrolysis combined with glycosylation increased β-type structures of SPI and solubility. Meanwhile, the DPY prepared by partially replacing milk protein with glycosylated SPI after enzymatic hydrolysis pretreatment for 40 min exhibited no statistically significant difference in texture and WHC with traditional yogurt while rheological properties were improved. The improvement of physical and chemical properties (TA, particle size, and zeta potential) and texture properties (hardness and consistency) confirmed the formation of a dense gel network structure observed in the microstructure. Glycosylated SPI after enzymatic hydrolysis pretreatment degraded the beany flavor and slightly bitter taste in DPY. Therefore, enzymatic hydrolysis pretreatment combined with glycosylation of SPI is an effective way to prepare DPY. While this study provides a theoretical basis for formulating emerging yogurt products in the future, further research is required to comprehensively evaluate its

functional properties.

Funding

This work was supported by the Key and R&D projects in Shandong Province [2022CXGC010603], Heilongjiang Province million project [2021ZX12B02], "14th Five-Year Plan" National Key Research and Development Plan [2021YFD2100401], and the Youth Leading Talent Support Plan of Northeast Agricultural University in 2023 [NEAU2023QNLJ-007] funded this research.

CRediT authorship contribution statement

Mengya Sun: Writing – original draft, Formal analysis, Data curation. **Zhenhai Yu:** Writing – review & editing. **Shuo Zhang:** Project administration, Investigation. **Caihua Liu:** Writing – review & editing. **Zengwang Guo:** Writing – review & editing, Visualization, Methodology, Investigation. **Jing Xu:** Project administration. **Guofang Zhang:** Writing – review & editing. **Zhongjiang Wang:** Project administration, Investigation.

Declaration of competing interest

The authors declare that they have no known competing financial interests or personal relationships that could have appeared to influence the work reported in this paper.

Data availability

Data will be made available on request.

References

Alkobeisi, F., Varidi, M. J., Varidi, M., & Nooshkam, M. (2022). Quinoa flour as a skim milk powder replacer in concentrated yogurts: Effect on their physicochemical, technological, and sensory properties. *Food Science & Nutrition, 10*(4), 1113–1125. https://doi.org/10.1002/fsn3.2771

Chen, B., Zhao, X., Cai, Y., Jing, X., Zhao, M., Zhao, Q., & Van der Meeren, P. (2023). Incorporation of modified okara-derived insoluble soybean fiber into set-type yogurt: Structural architecture, rheological properties and moisture stability. *Food Hydrocolloids, 137*, Article 108413. https://doi.org/10.1016/j.foodhyd.2022.108413

Chen, X., Zhao, H., Wang, H., Xu, P., Chen, M., Xu, Z., Wen, L., Cui, B., Yu, B., Zhao, H., Jiao, Y., & Cheng, Y. (2022). Preparation of high-solubility rice protein using an ultrasound-assisted glycation reaction. *Food Research International, 161*, Article 111737. https://doi.org/10.1016/j.foodres.2022.111737

Cheng, T., Wang, Z., Sun, F., Liu, H., Liu, J., Guo, Z., & Zhou, L. (2024). Gel properties of rice proteins-pectin composite and the delivery potential for curcumin: Based on different concentrations and the degree of esterification of pectin. *Food Hydrocolloids, 146*, Article 109305. https://doi.org/10.1016/j.foodhyd.2023.109305

Dai, Y., Li, H., Liu, X., Wu, Q., Ping, Y., Chen, Z., & Zhao, B. (2023). Effect of enzymolysis combined with Maillard reaction treatment on functional and structural properties of gluten protein. *International Journal of Biological Macromolecules, 128591*. https://doi.org/10.1016/j.ijbiomac.2023.128591

El-Kholy, W. M., Soliman, T. N., & Darwish, A. M. G. (2019). Evaluation of date palm pollen (*Phoenix dactylifera* L.) encapsulation, impact on the nutritional and functional properties of fortified yoghurt. *PLoS One, 14*(10), Article e0222789. https://doi.org/10.1371/journal.pone.0222789

Fan, L., Li, L., Xu, A., Huang, J., & Ma, S. (2022). Impact of fermented wheat bran dietary Fiber addition on dough rheological properties and noodle quality. *Frontiers in Nutrition, 9*, Article 952525. https://doi.org/10.3389/fnut.2022.952525

Ke, C., & Li, L. (2023). Influence mechanism of polysaccharides induced Maillard reaction on plant proteins structure and functional properties: A review. *Carbohydrate Polymers, 302*, Article 120430. https://doi.org/10.1016/j.carbpol.2022.120430

Klost, M., Giménez-Ribes, G., & Drusch, S. (2020). Enzymatic hydrolysis of pea protein: Interactions and protein fractions involved in fermentation induced gels and their influence on rheological properties. *Food Hydrocolloids, 105*, Article 105793. https://doi.org/10.1016/j.foodhyd.2020.105793

Kong, X., Li, X., Wang, H., Hua, Y., & Huang, Y. (2008). Effect of lipoxygenase activity in defatted soybean flour on the gelling properties of soybean protein isolate. *Food Chemistry, 106*(3), 1093–1099. https://doi.org/10.1016/j.foodchem.2007.07.050

Lei, M., Huang, J., Tian, X., Zhou, P., Zhu, Q., Li, L., Li, L., Ma, S., & Wang, X. (2021). Effects of insoluble dietary fiber from wheat bran on noodle quality. *Grain & Oil Science and Technology, 4*(1), 1–9. https://doi.org/10.1016/j.gaost.2020.11.002

Li, L., He, H., Wu, D., Lin, D., Qin, W., Meng, D., Yang, R., & Zhang, Q. (2021). Rheological and textural properties of acid-induced soybean protein isolate gel in the presence of soybean protein isolate hydrolysates or their glycosylated products. *Food Chemistry, 360*, Article 129991. https://doi.org/10.1016/j.foodchem.2021.129991

Liu, B., Li, N., Chen, F., Zhang, J., Sun, X., Xu, L., & Fang, F. (2022). Review on the release mechanism and debittering technology of bitter peptides from protein hydrolysates. *Comprehensive Reviews in Food Science and Food Safety, 21*(6), 5153–5170. https://doi.org/10.1111/1541-4337.13050

Liu, L., Li, Y., Prakash, S., Dai, X., & Meng, Y. (2018). Enzymolysis and glycosylation synergistic modified ovalbumin: Functional and structural characteristics. *International Journal of Food Properties, 21*(1), 395–406. https://doi.org/10.1080/10942912.2018.1424198

Martin, A. H., De los Reyes Jiménez, M. L., & Pouvreau, L. (2016). Modulating the aggregation behaviour to restore the mechanical response of acid induced mixed gels of sodium caseinate and soy proteins. *Food Hydrocolloids, 58*, 215–223. https://doi.org/10.1016/j.foodhyd.2016.02.029

Mehta, A., Kumar, L., Serventi, L., Schlich, P., & Torrico, D. D. (2023). Exploring the textural dynamics of dairy and plant-based yoghurts: A comprehensive study. *Food Research International, 171*, Article 113058. https://doi.org/10.1016/j.foodres.2023.113058

Metry, W., & Owayss, A. (2009). *T Influence of incorporating honey and royal jelly on the quality of yoghurt during storage. 37* pp. 115–131).

Muncan, J., Tei, K., & Tsenkova, R. (2020). Real-time monitoring of yogurt fermentation process by Aquaphotomics near-infrared spectroscopy. *Sensors (Basel, Switzerland), 21*(1), 177. https://doi.org/10.3390/s21010177

Nanakali, N. M., Muhammad Al-saadi, J., & Sulaiman Hadi, C. (2023). Functional and physiochemical properties of the yoghurt modified by heat lactosylation and microbial transglutaminase cross-linking of milk proteins. *Food Science & Nutrition, 11*(2), 722–732. https://doi.org/10.1002/fsn3.3108

Pang, Z., Xu, R., Zhu, Y., Bansal, N., & Liu, X. (2020). Tribo-rheology and kinetics of soymilk gelation with different types of milk proteins. *Food Chemistry, 311*, Article 125961. https://doi.org/10.1016/j.foodchem.2019.125961

Panyam, D., & Kilara, A. (1996). Enhancing the functionality of food proteins by enzymatic modification. *Trends in Food Science & Technology, 7*(4), 120–125. https://doi.org/10.1016/0924-2244(96)10012-1

Parandi, E., Mousavi, M., Assadpour, E., Kiani, H., & Jafari, S. M. (2024). Sesame protein hydrolysate-gum Arabic Maillard conjugates for loading natural anthocyanins: Characterization, in vitro gastrointestinal digestion and storage stability. *Food Hydrocolloids, 148*, Article 109490. https://doi.org/10.1016/j.foodhyd.2023.109490

Prasad, N., Thombare, N., Sharma, S. C., & Kumar, S. (2022). Gum arabic – A versatile natural gum: A review on production, processing, properties and applications. *Industrial Crops and Products, 187*, Article 115304. https://doi.org/10.1016/j.indcrop.2022.115304

Ren, Y., & Li, L. (2022). The influence of protease hydrolysis of lactic acid bacteria on the fermentation induced soybean protein gel: Protein molecule, peptides and amino acids. *Food Research International, 156*, Article 111284. https://doi.org/10.1016/j.foodres.2022.111284

Shen, P., Zhou, F., Zhang, Y., Yuan, D., Zhao, Q., & Zhao, M. (2020). Formation and characterization of soy protein nanoparticles by controlled partial enzymatic hydrolysis. *Food Hydrocolloids, 105*, Article 105844. https://doi.org/10.1016/j.foodhyd.2020.105844

Shen, X., Zhao, C., Lu, J., & Guo, M. (2018). Physicochemical properties of whey-protein-stabilized Astaxanthin Nanodispersion and its transport via a Caco-2 monolayer. *Journal of Agricultural and Food Chemistry, 66*(6), 1472–1478. https://doi.org/10.1021/acs.jafc.7b05284

Sun, J., Mu, Y., Mohammed, O., Dong, S., & Xu, B. (2020). Effects of single-mode microwave heating and dextran conjugation on the structure and functionality of ovalbumin–dextran conjugates. *Food Research International, 137*, Article 109468. https://doi.org/10.1016/j.foodres.2020.109468

Surrey, K. (1964). Spectrophotometric method for determination of Lipoxidase activity. *Plant Physiology, 39*(1), 65–70. https://doi.org/10.1104/pp.39.1.65

Victorino da Silva Amatto, I., Gonsales da Rosa-Garzon, N., Antônio de Oliveira Simões, F., Santiago, F., … Cabral, H. (2022). Enzyme engineering and its industrial applications. *Biotechnology and Applied Biochemistry, 69*(2), 389–409. https://doi.org/10.1002/bab.2117

Wang, F., Fan, W., Wang, B., Han, Y., & Sun, X. (2023). Characterizing acidified and renneted gels with different soy milk and skim milk proportions. *Food Research International, 172*, Article 113207. https://doi.org/10.1016/j.foodres.2023.113207

Wang, R., Wang, L.-H., Wen, Q.-H., He, F., Xu, F.-Y., Chen, B.-R., & Zeng, X.-A. (2023). Combination of pulsed electric field and pH shifting improves the solubility, emulsifying, foaming of commercial soy protein isolate. *Food Hydrocolloids, 134*, Article 108049. https://doi.org/10.1016/j.foodhyd.2022.108049

Wang, W., Hu, C., Sun, H., Zhao, J., Xu, C., Ma, Y., … Hou, J. (2022). Physicochemical properties, stability and texture of soybean-oil-body-substituted low-fat mayonnaise: Effects of thickeners and storage temperatures. *Foods, 11*(15), 2201. https://doi.org/10.3390/foods11152201

Wei, G., Dai, X., Zhao, B., Li, Z., Tao, J., Wang, T., & Huang, A. (2023). Structure-activity relationship of exopolysaccharides produced by *Limosilactobacillus fermentum* A51 and the mechanism contributing to the textural properties of yogurt. *Food Hydrocolloids, 144*, Article 108993. https://doi.org/10.1016/j.foodhyd.2023.108993

Xu, J., Xu, X., Yuan, Z., Hua, D., Yan, Y., Bai, M., Song, H., Yang, L., Zhu, D., Liu, J., Huo, D., & Liu, H. (2022). Effect of hemp protein on the physicochemical properties and flavor components of plant-based yogurt. *LWT, 172*, Article 114145. https://doi.org/10.1016/j.lwt.2022.114145

Yang, Y., Zhang, R., Zhang, F., Wang, B., & Liu, Y. (2022). Storage stability of texture, organoleptic, and biological properties of goat milk yogurt fermented with probiotic bacteria. *Frontiers in Nutrition, 9*, Article 1093654. https://doi.org/10.3389/fnut.2022.1093654

Zang, J., You, H., Li, S., Zhang, Y., Xu, H., Tang, D., Wu, S., Yao, Y., Tu, Y., & Yin, Z. (2023). Interpreting the "twice gelation" mechanism of a novel egg-based yoghurt through the dynamics of rheology, microstructure, and intermolecular forces. *Food Bioscience, 56*, Article 103318. https://doi.org/10.1016/j.fbio.2023.103318

Zha, F., Dong, S., Rao, J., & Chen, B. (2019). The structural modification of pea protein concentrate with gum Arabic by controlled Maillard reaction enhances its functional properties and flavor attributes. *Food Hydrocolloids, 92*, 30–40. https://doi.org/10.1016/j.foodhyd.2019.01.046

Zhang, Q., Li, L., Chen, L., Liu, S., Cui, Q., & Qin, W. (2023). Effects of sequential Enzymolysis and glycosylation on the structural properties and antioxidant activity of soybean protein isolate. *Antioxidants, 12*(2), Article 2. https://doi.org/10.3390/antiox12020430

Zhao, C., Chu, Z., Mao, Y., Xu, Y., Fei, P., Zhang, H., Xu, X., Wu, Y., Zheng, M., & Liu, J. (2023). Structural characteristics and acid-induced emulsion gel properties of heated soy protein isolate–soy oligosaccharide glycation conjugates. *Food Hydrocolloids, 137*, Article 108408. https://doi.org/10.1016/j.foodhyd.2022.108408

Zhong, L., Ma, N., Wu, Y., Zhao, L., Ma, G., Pei, F., & Hu, Q. (2019). Characterization and functional evaluation of oat protein isolate-Pleurotus ostreatus β-glucan conjugates formed via Maillard reaction. *Food Hydrocolloids, 87*, 459–469. https://doi.org/10.1016/j.foodhyd.2018.08.034